ARCHIVES of FOUNDRY ENGINEERING

ISSN (1897-3310)
Volume 10
Issue 2/2010

13 – 18

2/2

Published quarterly as the organ of the Foundry Commission of the Polish Academy of Sciences

The ATD thermal analysis of selected nickel superalloys

F. Binczyk*, J. Śleziona
Chair of Materials Technology
Silesian University of Technology, Krasińskiego Str. 8, 40-019 Katowice, Poland
*Corresponding author: E-mail address: franciszek.binczyk@polsl.pl

Received 08.03.2010; accepted in revised form 10.05.2010

Abstract

The study presents the results of the ATD thermal analysis made on selected nickel alloys used by WSK Rzeszów for parts of aircraft engines. The aim of the studies was investigation of solidification parameters, especially T_{lik} and T_{sol}. The said parameters are very important in the determination of pouring temperature and maximum operating temperature of castings. Another important technical information is the quality of "master heat" ingots, examined for the stability of chemical composition and presence of different impurities. It has been concluded that the pouring temperature of CMSX-4 and MAR-247 alloys should be comprised in a range from 1470 to 1480°C, while for the remaining alloys the recommended range of pouring temperatures is from 1440 to 1450°C. Examinations have also proved that some batches of the supplied ingots are contaminated with non-metallic impurities, located mainly in the region of shrinkage cavities.

Keywords: ATD Thermal Analysis, Nickel Superalloys, Solidification Parameters, Impurities

1. Introduction

The utilisation properties of cast parts depend on the structure formed during casting solidification and cooling. One of the tools used in the examination of these phenomena is ATD thermal analysis [1÷4]. The formation of casting structural constituents is an exothermic process, related with the precipitation of higher or lower volumes of energy. In the curves plotted by ATD thermal analysis, i.e. T=f(t) and dT/dt, the said changes assume the form of temperature-related collapses, inflections and arrests. The most important solidification parameters, typical of each cast alloy, include the liquidus temperature T_{lik}, responsible for the precipitation of the first crystals of a solid phase, and the solidus temperature T_{sol}, corresponding to the solidification of the last fraction of a liquid phase. The temperature T_{lik} is mainly used to determine an optimum value of the pouring temperature, and to ensure the sufficient alloy castability, the lowest possible shrinkage in volume, and the gas and non-metallic inclusions solubility reduced to minimum. On the other hand, the temperature T_{sol} provides information on the casting behaviour at high temperatures and on the optimum temperature of heat treatment. Within the range of alloy solidification temperatures, various eutectics can precipitate, usually shortly before the end of solidification process. The low-melting point complex eutectics have an adverse effect on the high-temperature casting performance properties, especially during heat treatment. If this is the case, melting and secondary dissolution in alloy matrix of the constituents of these eutectics can lead to a severe increase of microshrinkage porosity.

One of the main advantages that the ATD method of thermal analysis offers is a very short time during which the data on the tested material can be collected. With the production process going on, within the time of a few minutes only, it can be stated if the examined material has the required technological parameters or not. Basing on the results of this analysis, when done under industrial conditions, and on the measured casting

properties, some empirical relationships have been derived between the alloy solidification parameters (T_{lik}, T_{sol}, the values of dT/dt, the solidification time, etc.), the chemical composition and properties [5÷7].

2. Research problem

The T=f(t) curve and its derivative dT/dt (both generally known under the name of ATD curves) describe the processes of the nucleation and precipitation of primary phases, the crystallisation of metal matrix and eutectic, and phase transformations taking place in solid state. For most alloys, the plotted diagrams show four main stages of the solidification process. These stages are illustrated in Fig. 1 for a cylinder of φ40x100 mm cast from the IN-713C alloy.

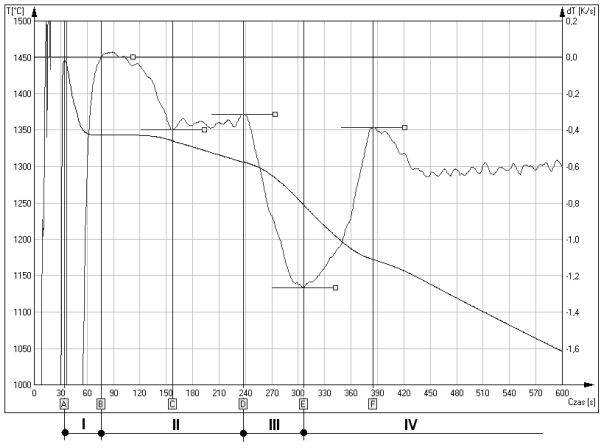

Fig. 1. The main stages of the solidification and cooling process observed in casting made from IN-713C alloy

Stage I, from T_{max} to T_{lik} (points A to B). The ATD curves provide information on the nucleation process, including the effect of modification (the formation of crystallisation nuclei) and the precipitation of primary phases (e.g. intermetallic phases and carbides).

Stage II, from T_{lik} to T_{Eut} (points B to D). The ATD curves are used in quantitative evaluation of the metal matrix composition (the content of γ phase, the eutectic containing carbides or intermetallic phases), helpful in predicting the mechanical properties of the examined alloy [10]. In this case, however, a calorimetric curve is also required to calculate the solidification heat of individual phase constituents.

Stage III, from T_{Eut} to T_{sol} (points D and E). The ATD curves help to evaluate the alloy "purity". Usually, the presence of gas and impurities in alloys results in the formation of low-melting point eutectic, which considerably prolongs the final stage of solidification and reduces the value of dT/dt derivative (the temperature drop rate). The slope of a tangent to the derivative also changes in function of the impurities content. When the slope of dT/dt curve decreases, a high degree of the alloy contamination with low-melting point non-metallic inclusions should be expected. The slope exceeding 70^o indicates alloys of high purity.

Stage IV, from T_{sol} to T_{ot} (from point E). The ATD curves illustrate the solid state phase transformations. In the case of IN-713C alloy (Fig. 2), the curve shows the γ to γ' transformation (structure ordering). A maximum of this transformation falls to point F (the maximum volume of emitted heat).

Even a rough estimate of the nickel alloys solidification process indicates that ATD thermal analysis is a tool very helpful in this respect and is recommended for use when the „master heat" ingots quality is evaluated [8].

3. Materials and methods of investigation

The solidification parameters were evaluated by ATD thermal analysis for the following nickel alloys: IN-713C, IN-100 and MAR-247, RENE-77 and CMSX-4.

Besides nickel, the chief constituents in these alloys are the following elements:

- IN-713C: 0,03% Co, 13,26% Cr, 5,85% Al, 4,10% Mo, 0,85% Ti, 2,27% (Nb + Ta).
- IN-100: 13,47% Co, 8,52% Cr, 5,76% Al, 2,98% Mo, 4,69% Ti, 0,82% V.
- MAR-M247: 10,01% Co, 8,47% Cr, 5,63% Al, 0,69% Mo, 1,02% Ti, 10,07% W, 3,27% Ta, i 1,40% Hf.
- Rene 77: 14,49% Co, 14,28% Cr, 4,42% Al, 4,20% Mo, 3,38% Ti.
- CMSX-4: 9,6% Co, 6,4%, Cr, 5,64% Al, 0,6% Mo, 1,02% Ti, 6,5% Ta, 6,4% W, 2,9% Re, 0,1% Hf.

Alloys selected for investigations were remelted in Balzers VSG-02 induction furnace using an Al_20_3 crucible which, owing to very stable technological parameters, was suitable for melting of high-purity alloys. The charge weight was 1,2 kg. Melting was carried out under a vacuum of 10^{-3}. Before pouring, the furnace working space was rinsed with argon. Pouring was conducted under argon atmosphere at a pressure of about 900 hPa. The test casting was designed as a φ 30x120 mm rod with 40x45x17 mm riser. The temperature was measured at 1/3 of the casting height (counting from the bottom). The Pt-PtRh10 thermocouple wire of 0,5 mm thickness was enclosed with quartz tube. The ceramic moulds ready for tests (moulds were made by the investment process at WSK Rzeszów) and mould placed in the chamber of an induction furnace are shown in Fig. 2.

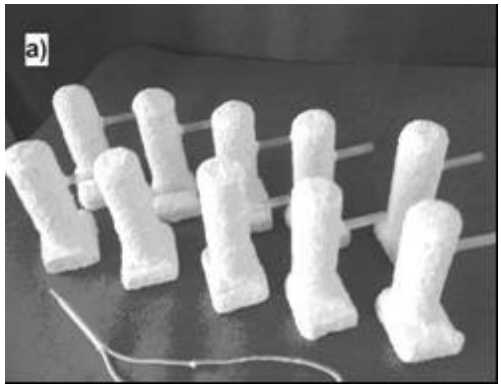

Fig. 2. Ceramic moulds ready for ATD analysis

Fig. 3. A view of the VSG-02 induction furnace

Basing on the values of the solidification parameters read out from the ATD curves, the best pouring temperatures were calculated for the examined alloys and their metallurgical purity was examined.

4. The results of investigations and discussion of results

The result of ATD analysis made on IN-713C alloy is shown as an example in Fig. 4.

The temperature values at predetermined characteristic points are as follows:

T_{max}	[A]	34 [s]	1446 [°C]
T_{wp}	[G]	46 [s]	1384 [°C]
T_{lik}	[B]	76 [s]	1343 [°C]
T_{Ep}	[C]	157 [s]	1335 [°C]
T_{Emax}	[D]	238 [s]	1306 [°C]
T_{sol}	[E]	306 [s]	1247 [°C]
T_{pst}	[F]	385 [s]	1172 [°C]

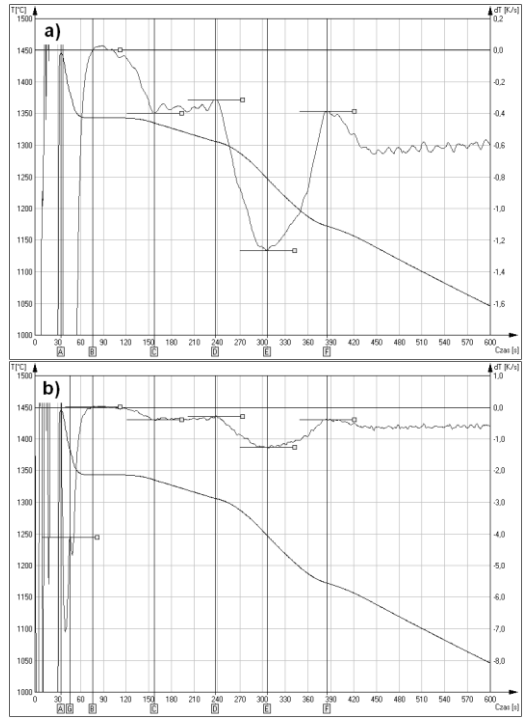

Fig. 4. The ATD derivative curve of IN-713C alloy plotted for the base units of 0,2°C/s (a) and 1,0°C/s (b)

Alloys subjected to thermal analysis differ from each other in type and/or content of the alloying elements, which have been typed in bold. Besides nickel content, each alloy has also additions of Cr, Al, Mo and Ti, and it can expected that the solidification course will largely depend on the content of these elements, especially as regards the initial temperature of the base alloy solidification process. Usually, before this stage, the nucleation and crystallisation of primary phases takes place; in most cases these are the intermetallic phases and primary carbides.

The derivative curves were plotted for two values of the base velocity unit, i.e. 0,2 ^{o}C/s and 1,0 ^{o}C/s. Lower values of the base unit enable more precise analysis of the changing values of the derivative, expressed by inflections and extrema. In this way, it becomes possible to determine with high accuracy the most important alloy solidification parameters, i.e. the temperatures T_{lik} and T_{sol}. When the value of the base unit is higher, it is possible to examine the crystallisation of primary phases, like carbides, intermetallic phases, and non-metallic inclusions of high melting point. The thermal effect appearing on the dT/dt curve due to the precipitation of a primary phase just before the beginning of the metal matrix solidification (phase γ) was observed in IN-713C (Fig. 4b – point G) and IN-100 alloys. The precipitation of these phases has occurred within the temperature range of 1380 to 1400^{o}C.

Reducing the recording time interval from 600 s to 240 s has considerably improved a correct interpretation of these effects, depicted for IN-100 alloy in Fig. 5.

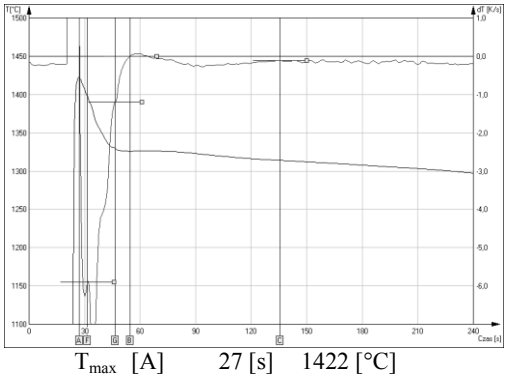

T_{max}	[A]	27 [s]	1422 [°C]
T_{wp1}	[F]	32 [s]	1398 [°C]
T_{wp}	[G]	47 [s]	1330 [°C]
T_{lik}	[B]	55 [s]	1326 [°C]
T_{Ep}	[C]	136 [s]	1314 [°C]

Fig. 5. The ATD derivative curve of IN-100 alloy plotted for the base unit of 0,2°C/s and the recording time interval reduced to 240 s

The plotted dT/dt curve shows additional collapses, which suggest the precipitation of other primary phases, e.g. at the temperature of 1330°C (point F). Most probably, these are the primary carbides of MC type, or unidentified so far high-melting point inclusions, or intermetallic phases.

No primary phases were observed to crystallise in CMSX-4 and RENE-77, and the reason can be very low carbon content kept in these alloys. Table 1 compares the temperatures of the precipitation of primary phases and of the beginning and end of alloy solidification to enable the choice of optimum pouring temperatures and heat treatment regime.

Table 1.
Solidification parameters of the examined alloys

Alloy	T_{wp}, °C	T_{lik}, °C	T_{Eut}, °C	T_{sol}, °C	T_{ps}, °C
IN-713C	1384	1343	1306	1247	1172
MAR-247	1366	1364	1350	1275	1212
RENE-77	-	1340	1281	1247	1101
CMSX-4	-	1380	1360	1303	1247
IN-100	1398, 1330	1326	1314	1355	1219

T_{ps} – temperature of γ to γ' transformation

From studies conducted so far the following conclusions have been drawn:

1. An empirical relationship can be established between the temperature T_{lik} and the content of main constituents present in the examined alloys. This refers in particular to alloys like Rene 77, IN-713C and IN-100. For MAR-257 the temperature T_{lik} is higher by 15 to 20°C, due to a 10% tungsten content in this alloy. The lowest temperature T_{lik} was observed in IN-100 as a result of Cr, Mo and Ti content reduced in respect of other alloys and Al content raised to a higher level.
2. The ATD curves indicate that before the crystallisation of the matrix takes place (T_{lik}), the primary intermetallic phases or carbides are precipitating from the liquid, acting as substrates for the crystal nucleation and growth in alloy matrix. Yet, the number of these precipitates is very scarce, as proved by an only insignificant change in temperature drop on the derivative curve. This is particularly well visible on the ATD curves plotted for IN-100, IN-713C and MAR-247. All these alloys contain carbon in an amount well above 0,15% C which, combined with the high content of alloying elements, can be the source of the formation of MC-type primary carbides. This conclusion, however, needs further confirmation by X-ray microanalysis.
3. Alloys examined currently are poured at temperatures from 1500 to 1520°C. As indicated by the results of thermal analysis, these temperatures are too high, especially for Rene77 and IN100.
4. From the investigations it follows that pouring temperature should be determined individually for each alloy. For CMSX-4 and MAR-247, this temperature should be comprised in a range from 1470 to 1480°C, while for other investigated alloys the recommended values are comprised in a range of 1440 to 1450°C.
5. For IN-713C and RENE-77, the temperature T_{sol} amounts to about 1247°C, which suggests the risk of surface melting of a carbide eutectic if the heat treatment is carried out at a temperature too high.

When alloys are melted, various impurities can penetrate into the melt. In most cases they originate from:

- contaminated charge materials,
- ceramic materials used for crucible,
- incorrect atmosphere in furnace chamber (e.g. argon contaminated with oxygen),
- products of reaction transferred from moulding material to molten alloy, especially at high pouring temperatures.

The technology of nickel alloys melting (closed melting chamber) makes refining, deslagging, etc. impossible. Therefore, each of the above mentioned factors may eventually lead to a contamination of these alloys with non-metallic inclusions or gas. The said effects can contribute to the formation of shrinkage porosities and non-metallic inclusions, especially on grain boundaries.

Most of the non-metallic inclusions are characterised by low solidification temperature, which makes them gather ahead of the solidification front and solidify as the last ones, i.e. at the solidification stage III (Fig. 1).

The analysis of dT/dt derivative curve, showing the rate of temperature drop during this period, helps in qualitative evaluation of the consequences of the alloy being contaminated with non-metallic inclusions and gas.

Figures 6 to 9 show examples of ATD curves plotted for the "master heat" ingots made from IN-713C (7V2124 and M3023) and MAR-247 (7V 2128 and 3V 4253), supplied by different producers.

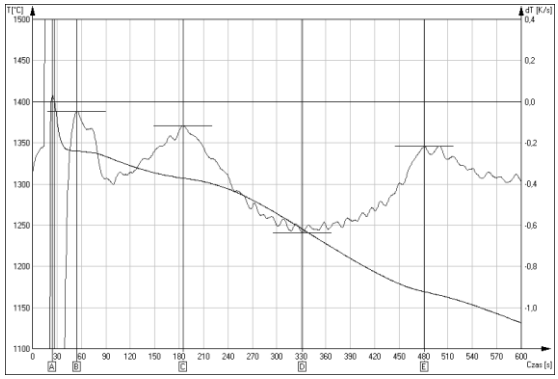

T_{max}	[A]	25 [s]	1408 [°C]
T_{lik}	[B]	55 [s]	1340 [°C]
T_E	[C]	185 [s]	1307 [°C]
T_{sol}	[D]	332 [s]	1245 [°C]
T_{ps}	[E]	482 [s]	1169 [°C]

$T_E - T_{sol} = 62°C$

$t_D - t_C = 147$ s

Fig. 6. ATD curve plotted for IN-713 C (7V2124)

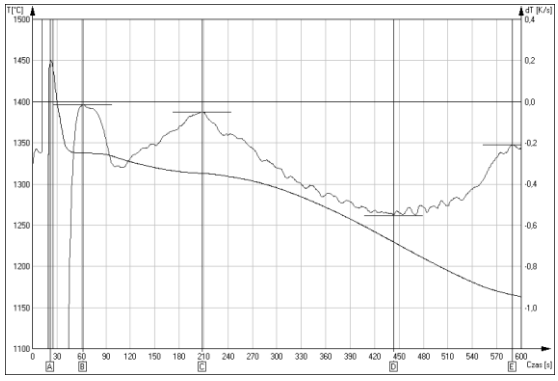

T_{max}	[A]	22,0 [s]	1450,0 [°C]
T_{lik}	[B]	62,0 [s]	1336,0 [°C]
T_E	[C]	209,0 [s]	1313,0 [°C]
T_{sol}	[D]	444,0 [s]	1230,0 [°C]
T_{ps}	[E]	590,0 [s]	1165,0 [°C]

$T_E - T_{sol} = 83^oC$

$t_D - t_C = 235$s

Fig. 7. ATD curve plotted for IN-713 C (M3023)

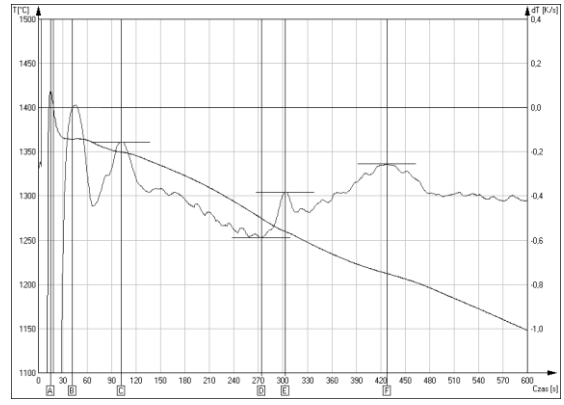

T_{max}	[A]	15 [s]	1418 [°C]
T_{lik}	[B]	42 [s]	1364 [°C]
T_E	[C]	101 [s]	1349 [°C]
T_{sol}	[D]	274 [s]	1275 [°C]
T_{pst-1}	[E]	303 [s]	1259 [°C]
T_{pst-2}	[F]	428 [s]	1213 [°C]

Fig. 8. ATD curve plotted for MAR-247 (7V 2128)

The presence in alloy of gas and impurities usually results in the formation of low-melting point eutectic, which considerably prolongs the final stage of solidification and reduces the value of dT/dt derivative (the rate of temperature drop). The slope of a tangent to the derivative also changes and depends on the alloy contamination rate. With the slope of dT/dt derivative decreasing, the alloy can have a very high content of the low-melting point non-metallic inclusions.

High slope, i.e. exceeding 70°, allows expecting an alloy of the sufficiently high purity.

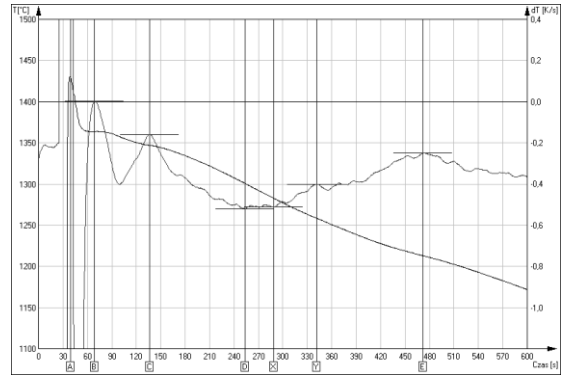

T_{max}	[A]	40 [s]	1429 [°C]
T_{lik}	[B]	70 [s]	1364 [°C]
T_E	[C]	137 [s]	1347 [°C]
T_{sol1}	[D]	254 [s]	1301 [°C]
T_{sol2}	[X]	289 [s]	1283 [°C]
T_{pst-1}	[Y]	342 [s]	1259 [°C]
T_{ps-2}	[E]	472 [s]	1213 [°C]

Fig. 9. ATD curve plotted for MAR-247 (3V 4253)

The results of ATD analysis made for the examined alloys at the solidification stage III are confirmed by surface examinations of the test ingots shown in Figs. 10 to 12.

a) b)

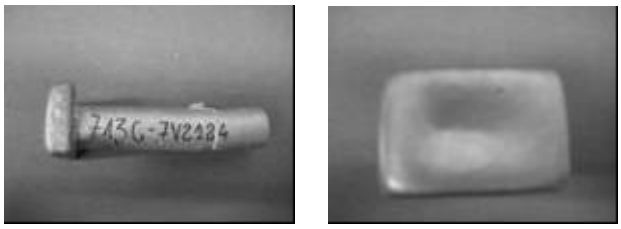

Fig. 10. Side and upper surface of test casting made from IN-713C (7V2124)

a) b)

Fig. 11. Side and upper surface of test casting made from IN-713C (M3023)

a) b)

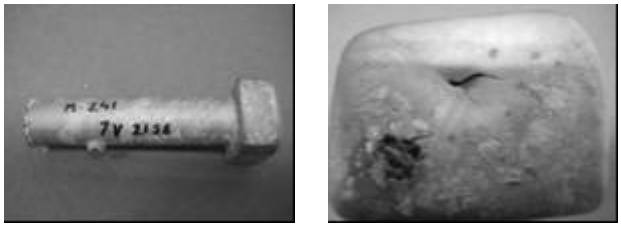

Fig. 12. Side and upper surface of test casting made from MAR-247 (3V 4253)

The conducted investigations enabled the following conclusions to be drawn:

1. IN713C (7V212) alloy
   The run of ATD curve is correct. The values of the temperatures T_{lik}, T_E , T_{sol} and T_{ps} are correct.
2. IN713C (M3023) alloy
   The run of the ATD curve indicates possible precipitation of non-metallic inclusions (long time elapsing till alloy solidification and low value of the derivative curve slope angle in the range of T_E to T_{sol}. The solidification range at stage III increased by 21°C and the time longer by 88s.
   The casting surfaces (top surface and upper side surfaces under the gate) are coated with numerous black spots (probably originating from the inclusions). In the central part of the supplied „master heat" ingot, a large cavity (a hole and porosities) is visible, gathering in its inside all inclusions. All characteristic temperatures are lower than they should be!
3. MAR-247 (3V4253) alloy
   The run of ATD curve is correct. The values of the temperatures T_{lik}, T_E , T_{sol} and T_{ps} are correct.
4. MAR-247 (7V2128) alloy
   The ATD curve slightly differs from the curves obtained so far. It is difficult to determine the temperature of the end of solidification T_{sol}, as it rather forms a "range" extending from point D to point X, which can prove the precipitation of additional eutectic. This statement has been confirmed by examinations of the casting surface, especially its upper part where large non-metallic inclusions (?) are observed. In the central part of the supplied „master heat" ingot, a large cavity (a hole and porosities) is visible, gathering in its inside all inclusions.

Acknowledgements

Financial support of Structural Funds in the **Operational Programme - Innovative Economy (IE OP)** financed from the European Regional Development Fund – Project No POIG.0101.02-00-015/08 is gratefully acknowledged.

References

[1] Rabus D., Wutzl K.: Quantitative Berechnung der Gesamtwärme von Schmelzen beim Erstarren und daraus folgende Überlegungen zur Entstehung von Chunky-Graphit, Giesseren-Rundschau, nr 6, 1975
[2] Longa W.: Elementarna teoria analizy różniczkowej krzywych stygnięcia odlewów, Metalurgia i Odlewnictwo, t. 10, 1984
[3] Jura S.: Krzywa kalorymetryczna w analizie termicznej i derywacyjnej procesu krystalizacji metali i stopów, Krzepnięcie Metali i Stopów, t. 14, PAN-Katowice, Komisja Odlewnicza, 1992
[4] Jura S., Jura Z.: Krzywa kalorymetryczna i źródło ciepła w analizie termicznej i derywacyjnej procesu krzepnięcia żeliwa, Krzepnięcie metali i Stopów, t. 16, PAN-Katowice, Komisja Odlewnicza, 1992
[5] Jura S., Sakwa J., Borek K.: Zastosowanie analizy termicznej i różniczkowej dla określenia parametrów składu chemicznego. Krzepnięcie Metali i Stopów, 2, 1980, PAN
[6] Binczyk F., Krzemień E.: Zastosowanie różniczkowych krzywych krzepnięcia w badaniach krystalizacji żeliwa, Mat. Konferencyjne "Krzepnięcie Metali i Stopów", PAN, Mechanika 23, Gliwice, 1980
[7] Pietrowski S., Władysiak R.: Kontrola metodą ATD siluminów tłokowych, Krzepnięcie Metali i Stopów, 28, PAN, Katowice, 1996
[8] Binczyk F., Śleziona J., Cwajna J., Roskosz S.: ATD and DSC analysis of nickel super alloys, Archives of Foundry Engineering Vol. 8, Issue 3, 2008, pp. 5-9